10498 *Macromolecules* **2010**, *43*, 10498–10504
DOI: 10.1021/ma102206f

Macromolecules
ARTICLE

Influence of the Degree of Sulfonation on the Structure and Dynamics of Sulfonated Polystyrene Copolymers

Alicia M. Castagna,[†] Wenqin Wang,[‡] Karen I. Winey,*[,‡] and James Runt*[,†]

[†]*Department of Materials Science and Engineering, The Pennsylvania State University, University Park, Pennsylvania 16802, United States, and* [‡]*Department of Materials Science and Engineering, University of Pennsylvania, Philadelphia, Pennsylvania 19104, United States*

Received September 23, 2010; Revised Manuscript Received November 17, 2010

ABSTRACT: The structure and dynamics of sulfonated polystyrene (SPS) acid copolymers were investigated using X-ray scattering and broadband dielectric relaxation spectroscopy (DRS). Evidence of acid group aggregation was found at 3.5, 6.7, and 9.5 mol % sulfonation. An increase in the segmental relaxation time and dielectric relaxation strength was observed with increasing acid content. The average state of dipolar interactions was quantified as a function of temperature using the Onsager equation and the Kirkwood−Fröhlich correlation factor. Two high-temperature relaxation processes at frequencies 4−7 decades below the segmental relaxation were identified and are proposed to originate from Maxwell−Wagner−Sillars interfacial polarization and association dynamics of various assemblies of acid groups.

Introduction

Ion-containing polymers are of interest in a variety of applications, ranging from high-performance coatings to ion transport for actuation and battery materials. Ionomers, copolymers with a small fraction ($<\sim$10%) of ionic functional groups, have been of interest since the 1960s owing to improved properties over their nonionic counterparts.[1,2] Incorporating even a small fraction of ionic groups has been found to dramatically change the physical properties. This property enhancement arises largely from the aggregation of these ionic groups that act as thermoplastic cross-links.

Despite the extensive prior research on ionomers, there still remain areas that are not well understood, particularly the correlation between ionic aggregate structure and chain dynamics. Sulfonated polystyrene in particular has been the model ionomer of choice for a number of investigations of morphology and dynamics using X-ray and neutron scattering,[3−7] rheology,[8,9] and dynamic mechanical analysis (DMA).[10,11] However, few of these studies attempt to directly correlate structure with dynamics. A thorough understanding of the structure−property relationships of these materials is critical to designing ionomers with desired mechanical or electrical properties.

This investigation will integrate the findings from several characterization methods including X-ray scattering, scanning transmission electron microscopy (STEM), and broadband dielectric relaxation spectroscopy (DRS) to provide a holistic approach to understanding the complex behavior of these materials. Sulfonated polystyrene was chosen as the model ionomer due to both its well-defined microphase-separated structure and its dynamic properties. Polystyrene provides a relatively inactive dielectric background, enabling the investigation of the dynamics due to the sulfonated groups using DRS. In a recent investigation, the dynamics of a sampling of SPS acid copolymers and ionomers were revealed to be quite complex; however, the morphology of the ionic aggregates in these studies was not well characterized.[12,13]

In a series of papers we will provide new insight into the dynamics of these materials through a systematic investigation of the effects of sulfonation, neutralizing ion type, and degree of neutralization on morphology and dynamics. The present paper focuses on the acid copolymers (SPS-H), which are precursors to the ionomers. Additionally, the critical role of thermal history will be addressed.

Experimental Methods

Sample Preparation. Nearly monodisperse atactic PS was purchased from Pressure Chemical (M_w = 123 kg/mol, PDI = 1.06). Sulfuric acid, acetic anhydride, and dichloromethane were obtained from Fisher Scientific. Sulfonated polystyrene acid copolymers (SPS-H) were prepared by sulfonation of polystyrene according to procedures described in the literature.[14] Acetyl sulfate was synthesized by combining concentrated sulfuric acid with a solution of acetic anhydride in dichloromethane with acetic anhydride in excess. Freshly prepared acetyl sulfate was added slowly into a gently agitated solution of polystyrene in dichloromethane at 40 °C. The sulfonation reaction proceeded for 4 h and was then terminated by the addition of methanol. The polymers were isolated by precipitation into methanol and then were washed several times with deionized water.

The level of sulfonation was determined by Atlantic Microlab (Norcross, GA) using elemental sulfur analysis by combustion (3.5, 6.7, and 9.5 mol %, subsequently referred to as SPS3.5, SPS6.7, and SPS9.5, respectively). These sulfonation levels were consistent with the results of titration experiments, in which methanol solutions of SPS were titrated with 0.01 M NaOH using the indicator thymol blue.

The acid copolymers were dried under vacuum at 80 °C for at least 3 days and then at 110−120 °C for 1−2 days. The copolymers SPS6.7 and SPS9.5 were further annealed at $\sim T_g$ + 20 °C for 24 h. Water content was determined by coulometric Karl Fischer (KF) titration using Hydranal CG and Hydranal AG-H as KF reagents. The samples were dissolved in chloroform before titration. The water contents of all three acid copolymers were found to be less than 0.3 wt % after drying and annealing. The dried films were then hot pressed at 150 °C

*To whom correspondence should be addressed.

 Published on Web 12/02/2010

and used for X-ray scattering and dielectric measurements. The absence of thermal degradation was verified (Supporting Information) using FTIR spectroscopy and DRS. All materials were stored in vacuum desiccators prior to characterization.

Thermal Analysis. Glass transition temperatures (T_g) were determined using a TA Instruments Q2000 differential scanning calorimeter. The response was measured over the temperature range 40−180 °C at a heating rate of 10 °C/min under a nitrogen flow of 50 mL/min. The T_g was taken as the inflection point in the DSC thermogram from the second heating scan.

Fourier Transform Infrared Spectroscopy (FTIR). Samples were prepared for FTIR experiments by hot pressing into thin films at 160 °C. Spectra were collected with a resolution of 2 cm^{-1} using a Nicolet 450 FTIR spectrometer equipped with a MCT/B detector. 256 scans were signal averaged for each sample at room temperature. Additional spectra were collected for SPS9.5 on cast films subjected to identical thermal treatment conditions as those investigated by SAXS and DRS to verify the absence of chemical changes or degradation due to thermal history (see Supporting Information, Figures S1 and S2).

X-ray Scattering. X-ray scattering experiments were performed with a multiangle X-ray scattering (MAXS) apparatus using Cu Kα X-rays generated from a Nonius FR 591 rotating-anode generator operated at 40 kV and 85 mA. The beam is focused by doubly focusing mirror-monochromator optics in an integral vacuum system. The scattering data were collected using a Bruker Hi-Star multiwire detector at sample-to-detector distances of 150, 54, and 11 cm. The isotropic 2-D data were integrated into 1D plots using Datasqueeze software.[15]

The scattering data of the SPS acid copolymers (where possible) were modeled using

$$I(q) = I_{KT}(q) + L_1(q) + L_2(q) + C \quad (1)$$

where $I_{KT}(q)$ is the Kinning−Thomas modified hard-sphere model[7,16] used to interpret the aggregate or "ionomer" peak, $L_1(q)$ and $L_2(q)$ are Lorentzian functions used to fit the two polystyrene-related peaks, and C is a constant used to account for the instrumental background scattering, as previously reported.[17] The Kinning−Thomas model is the modified version of the Yarusso−Cooper model,[4,7,16] where the Percus−Yevick[18] total correlation function that accounts for correlations between all particles in the system was used instead of the Fournet[19] three-body interference function.

The Kinning−Thomas model assumes that this scattering peak arises from interparticle scattering from monodisperse, spherical aggregates homogeneously distributed in the polymer matrix of lower electron density. This model utilizes four variable parameters to characterize aggregation: the radius of aggregates R_1, the radius of closest approach R_{CA}, the number density of the aggregates N_p, and the amplitude A of the scattering maxima.[7] Zhou et al. have demonstrated that for lightly sulfonated SPS ionomers the size and number density of ionic aggregates observed in high angle annular dark field (HAADF) STEM and determined from fitting the X-ray scattering data quantitatively agree.[7] Previously, Benetatos et al. used this scattering model to reconcile HADDF STEM and X-ray scattering in poly(ethylene−methacrylic acid) ionomers.[17,20]

Broadband Dielectric Relaxation Spectroscopy. Isothermal relaxation spectra were collected under nitrogen using a Novocontrol GmbH Concept 40 DRS spectrometer from 0.01 Hz to 10 MHz on heating from 10 to 220 °C. Additional cooling scans were collected to ensure reversibility and the absence of degradation. Samples with thicknesses of 0.2−0.4 mm were sandwiched between brass electrodes with a top electrode diameter of 2 cm.

Dielectric strength ($\Delta\varepsilon$) and characteristic relaxation time (τ_{HN}) are determined for each relaxation process by fitting the dielectric loss (ε^*) to the appropriate form of the Havriliak−Negami (HN) function:

$$\varepsilon^*(\omega) = \frac{\Delta\varepsilon}{(1 + (i\tau_{HN}\omega)^a)^b} \quad (2)$$

where a and b are shape parameters. The characteristic relaxation time is related to the frequency of maximum loss by

$$f_{max} = \left[\frac{1}{2\pi\tau_{HN}}\right]\left[\frac{\sin(\pi a/(2+2b))}{\sin(\pi ab/(2+2b))}\right]^{1/a} \quad (3)$$

At temperatures above T_g ohmic conduction due to charge carriers frequently dominates the loss contribution (ε''), effectively masking dipolar processes. This conduction contribution is not manifested in the real part of the dielectric response (ε'). The real and imaginary components of the dielectric constant contain the same information and are described by the Kramers−Kronig relations. Using a numerical approach, we can calculate the conduction-free dielectric loss from the real part of the dielectric constant revealing additional processes at high temperatures. There are several numerical methods to achieve this, including the Kramers−Kronig transform which requires numerical approximation and interpolation. A more straightforward alternative is a derivative method, where the conduction-free dielectric loss, ε''_D, is determined from the logarithmic derivative of the real part of the dielectric constant:[21,22]

$$\varepsilon''_D = -\frac{\pi}{2}\frac{\partial\,\varepsilon'(\omega)}{\partial \ln \omega} \quad (4)$$

Wubbenhorst et al. have shown that this method is a very good approximation for calculating the conduction-free dielectric loss.[21,22] This derivative method has the added advantage of sharpening peaks which aids in the resolution of adjacent processes.[21,22] Appropriate forms of the HN function were used to fit peaks resolved by this method.[22]

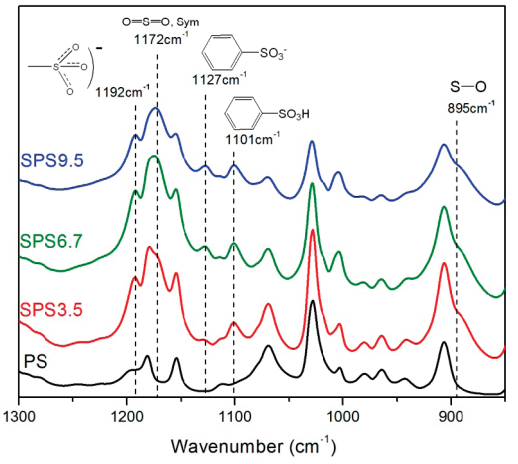

Figure 1. FTIR absorbance spectra of PS, SPS3.5, SPS6.7, and SPS9.5 in the region from 850 to 1300 cm^{-1}. Data are shifted vertically for clarity.

Results and Discussion

Room Temperature Structure. FTIR was used to confirm the structure of SPS as well as to probe the association state of the sulfonic acid groups at room temperature. A portion of the spectra for PS and the sulfonated copolymers are shown in Figure 1 with peaks of particular interest highlighted. The band at 1192 cm^{-1} is assigned to the antisymmetric stretching of the sulfonate ion.[12,23] The sulfur−oxygen bond stretching

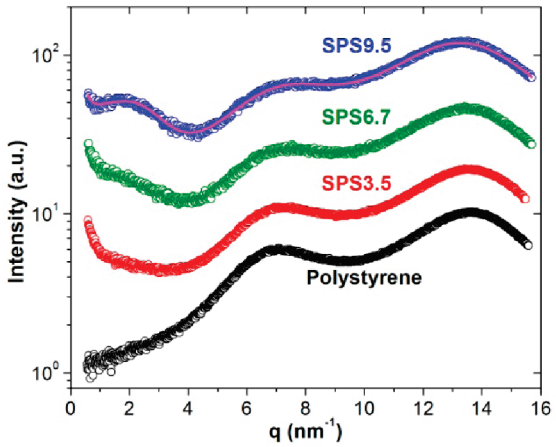

Figure 2. Room temperature X-ray scattering intensity vs scattering vector q for PS, SPS3.5, SPS6.7, and SPS9.5. The line is the best fit of eq 1 to the scattering data from SPS9.5. Data are shifted vertically for clarity.

vibration with single- and double-bond character is evidenced by the bands at 895 and 1172 cm^{-1}, respectively.[12,23] Two distinct bands are observed for the in-plane skeletal vibration of the benzene ring substituted with SO_3^- (1127 cm^{-1}) and SO_3H (1101 cm^{-1}).[12,23]

The existence of SO_3^- bands (1127 cm^{-1}) was unexpected because it indicates dissociated or "free" anions. This peak likely originates from charge delocalization within the sulfonic acid aggregates which effectively screens the influence of the proton on the skeletal vibrations of the benzene ring, resulting in anions that appear "free". The relative intensity of this band increases with increasing sulfonation, thereby reflecting a more defined state of aggregation with increasing acid content.

The scattering profiles for PS and the annealed acid copolymers are shown in Figure 2. Three isotropic maxima are observed for SPS9.5: the polystyrene amorphous halo (~13 nm^{-1}), polystyrene "polymerization peak" (~7 nm^{-1}), and a third scattering maxima (~2 nm^{-1}). The two higher angle maxima are typical features in the scattering patterns of amorphous polystyrene.[24] The third is at a similar position as the ionomer peak typically observed for SPS ionomers and indicates the assembly of acid groups in this copolymer. The scattering profile of SPS9.5 was successfully fit to eq 1 with the following parameters from the K−T model: R_1 = 0.79 nm, R_{CA} = 0.98 nm, N_p = 0.0214 nm^{-3}. This model failed to adequately fit the weaker acid aggregation scattering in SPS3.5 and SPS6.7 due to peak broadness and the small-angle upturn. Both SPS3.5 and SPS6.7 exhibit excess scattering at $q \sim 2$ nm^{-1}. This along with the "free" anion band (1127 cm^{-1}) in the FTIR spectra indicates that acid groups in these copolymers have assembled.

Evidence of acid group assembly from scattering experiments is not unprecedented.[4,5,25] Yarusso et al. observed this peak in their study of SPS ionomers and their acid precursors (1.6, 3.4, 5.6, and 6.9 mol % sulfonated repeat units); however, it was later suggested by Weiss et al. that residual solvent was the source of improved contrast in their scattering profile.[4,5] While Weiss et al. did not observe this scattering maxima for SPS containing 1.8 or 5.8 mol % sulfonic acid groups, there was evidence of microphase separation from dynamic mechanical analysis experiments.[5]

Effect of Processing and Temperature on Structure. To ascertain the state of aggregation in these acid copolymers, X-ray scattering profiles were acquired after each processing

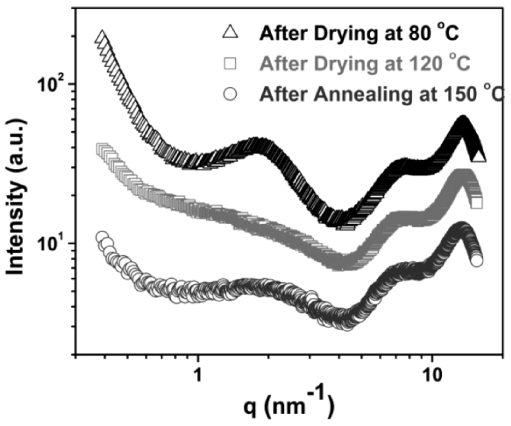

Figure 3. Room temperature X-ray scattering results from the SPS9.5 acid copolymer showing the effect of thermal history. Data are shifted vertically for clarity.

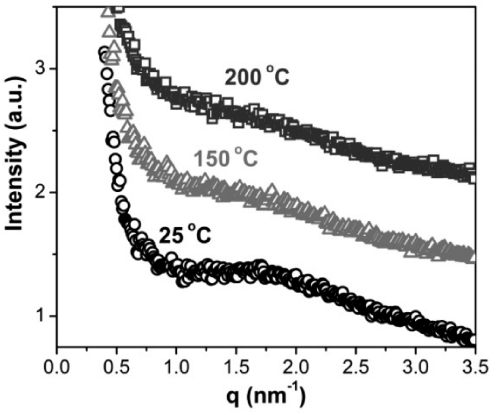

Figure 4. X-ray scattering profiles of SPS9.5 at 25, 150, and 200 °C. Plots are shifted vertically for clarity.

step (Figure 3). Using Karl Fischer titration, the water content after annealing at 80 and 120 °C are 1.2 and 0.66 wt %, respectively. Thus, the strong low angle (~2 nm^{-1}) peak found after drying at 80 °C is apparently the result of excess water, as suggested by Weiss et al.[5] Interestingly, after annealing above T_g the aggregation peak recovers despite further reduction in water content (< 0.3 wt %). We propose that prior to annealing the acid groups are in a nonequilibrium state. Upon heating above T_g the acid groups have sufficient thermal energy to aggregate in a more favorable microphase-separated structure with a better defined interaggregate spacing. This is yet another illustration of the critical role of sample history and preparation on the microstructure of these materials. Note that a critical attribute of this study is that precisely the same samples were used for FTIR, X-ray scattering, and DRS experiments.

Determining the state of the acid groups and their assemblies at high temperatures is critical for our comparison to the dynamics. The annealed samples were investigated using X-ray scattering at elevated temperatures, and it was found that the aggregation peak broadens with increasing temperature, as is illustrated in Figure 4 for SPS9.5. This broadening is likely a result of the transition from a static cross-linked system to a dynamic network. As the temperature is increased, the lifetime of a sulfonic acid group in an aggregate is expected to decrease due to increased randomization caused by more thermal energy.

Segmental Dynamics. Segmental relaxation arises from the cooperative motion of chain segments and is related to the

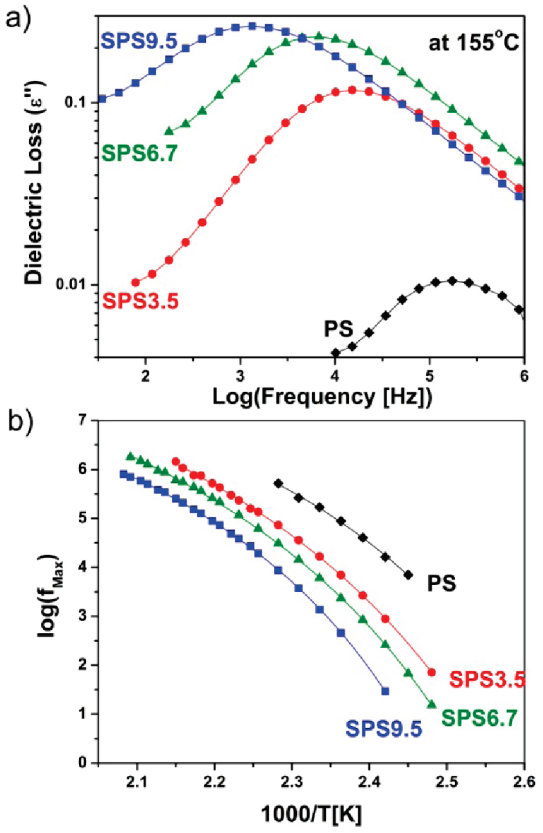

Figure 5. (a) Dielectric loss spectra at 155 °C showing the segmental relaxation of PS, SPS3.5, 6.7, and 9.5. Lines are included to guide to the eye. (b) Temperature dependence of the segmental relaxation time for PS, SPS3.5, 6.7, and 9.5. Lines are fits to the VFT equation (eq 5).

Table 1. Dynamic T_g (T_{ref}) from DRS and Calorimetric T_g from DSC for PS, SPS3.5, SPS6.7, and SPS9.5

	$T_{ref} \pm 10$ (°C)	$T_g \pm 3$ (°C)
PS	97	107
SPS3.5	105	111
SPS6.7	110	117
SPS9.5	120	121

glass transition. A significant shift to lower frequencies is observed with increasing sulfonation content at all accessible temperatures (Figure 5a,b). This slowing down is due to increasing steric hindrance from the addition of sulfonic acid groups to the chain backbone and restrictions due to acid group−acid group associations.

The maximum relaxation frequencies of the segmental process (Figure 5b) follow a Vogel−Fulcher−Tamman temperature dependence as expected:

$$f = f_0 \exp\left(\frac{B}{T - T_0}\right) \tag{5}$$

where T_0 is the Vogel temperature, f_0 is associated with vibration lifetimes,[26] and the temperature coefficient B is related to the apparent activation energy ($E_a = BR/(1 - T_0/T)^2$).[21] The dynamic T_g (T_{ref}) can be determined from the segmental relaxation by extrapolating the VFT fit of the relaxation frequency maxima to $\tau = 100$ s. T_{ref} and the calorimetric T_g are within error (Table 1).

The fragility, or deviation from Arrhenius behavior, yields additional information about the cooperative motion. The fragility index m can be calculated from the VFT fit parameters from the relation[27]

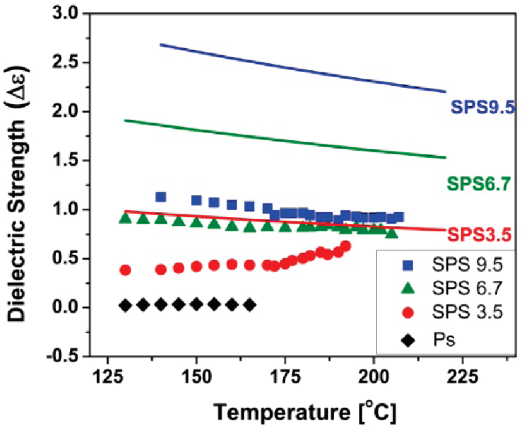

Figure 6. Temperature dependence of the measured dielectric strength (symbols) and the limiting case dielectric strength assuming $g = 1$ (lines).

$$m = \left.\frac{\mathrm{d}\log(\tau)}{\mathrm{d}(T_g/T)}\right|_{T=T_g} = \frac{B/T_g}{(\ln 10)(1 - T_0/T_g)^2} \tag{6}$$

The m values calculated, using $T_g = T_{ref}$, are within statistical error for PS, SPS3.5, SPS6.7, and SPS9.5. PS is relatively fragile with $m = 140$, which agrees with literature values.[26] Previous studies have revealed that the addition of H-bonding in already highly fragile polymers does not have a significant impact on cooperativity.[12,28] Atorngitawat et al. also did not observe an appreciable difference in fragility in their investigation of SPS acid copolymers.[12]

The dielectric strength of the segmental process is 1−2 orders of magnitude higher for the sulfonated polystyrenes compared to neat PS (Figure 6). The increase in strength naturally arises from the enhanced dipole moment imparted by the sulfonic acid groups; therefore, chain segments containing these moieties dominate the observed relaxation strength of the SPS α process. A better understanding of the origin of experimental dielectric strengths, $\Delta\varepsilon$, can be obtained by considering the Onsager equation:

$$\Delta\varepsilon = \frac{1}{3\varepsilon_0}\left(\frac{\varepsilon_s(\varepsilon_\infty + 2)^2}{3(2\varepsilon_s + \varepsilon_\infty)}\right) g \frac{\mu^2}{kT}\frac{N}{V} \tag{7}$$

where g ($g = \mu_{eff}^2/\mu_0^2$, where μ_{eff} and μ_0 are the condensed and gas phase dipole moments, respectively) is the Kirkwood−Fröhlich correlation factor which takes into account the orientational effects of short-range interactions between molecules,[29] N/V is the number density of sulfonic acid groups, ε_s and ε_∞ are the low- and high-frequency limits of the dielectric constant, and ε_0 is the permittivity of vacuum. The gas phase dipole moment was taken as a first approximation as that of benzenesulfonic acid (4.98 D) determined from ab initio calculations.[30] ε_∞ is determined from the square of the refractive index (n), $\varepsilon_\infty = n_2$.[31,32] In our calculations the refractive index of polystyrene is used.

For a limiting case we assume the contribution to the α process from polystyrene segments is negligible and that all sulfonic acid dipoles are free and noninteracting ($g = 1$). When compared with the experimental dielectric strengths, in Figure 6, it is apparent that the measured values are significantly lower. In addition, the predicted strengths increase proportionally with sulfonic acid content. The discrepancy

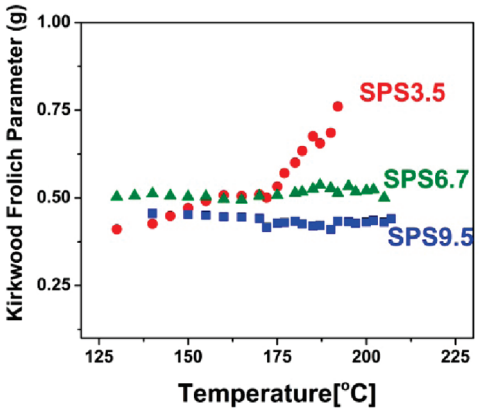

Figure 7. Temperature dependence on the Kirkwood−Fröhlich correlation factor (g) calculated from the experimental dielectric strength of SPS3.5, SPS6.7, and SPS9.5.

between the experimental results and the limiting case predictions arises from interacid associations. Sulfonic acid groups have been demonstrated to hydrogen bond into dimers.[8,33] Moreover, assemblies of sulfonic acid groups are present in these materials as evidenced by FTIR and X-ray scattering data, as presented above.

Because we do not know the precise state of acid association, i.e., the fraction of free vs associated and type of associations (dimers or larger scale aggregates), nor can we necessarily assume that the dipole moment of these assemblies is negligible, it is not possible to estimate the number of free vs aggregated dipoles from DRS. We can, however, estimate the interactions of neighboring dipoles using the Kirkwood−Fröhlich correlation factor.

The measured $\Delta\varepsilon$ in Figure 6 is used to determine the effective dipole moment (μ_{eff}) from the Onsager equation (eq 7) using the μ_0 value for benzenesulfonic acid. When $g = 1$ dipoles are not interacting, when $g > 1$ dipoles correlate in a parallel manner, and when $g < 1$ dipoles are correlate in an antiparallel arrangement. The calculated g factors for SPS3.5, SPS6.7, and SPS9.5 are all less than one (Figure 7), indicating that the effective dipole moment is reduced due to net antiparallel orientation of the hydrogen-bonded sulfonic acid groups. There is, however, a distribution in correlating orientations that is expected from acid groups associated in aggregates.

The temperature dependence of g in Figure 7 reflects the average state of association. For SPS6.7 and SPS9.5, the net associations remain essentially constant at the time scale of the segmental process from 125 to 205 °C. The increase in g for SPS3.5 indicates that the number of associated dipoles decreases with increasing temperature, rapidly around 170 °C. Thus, we conclude that the acid associations in SPS3.5 are predominately dimers that dissociate at higher temperatures due to thermal randomization. Meanwhile, the acid associations in SPS6.7 and SPS9.5 are probably larger, more stable aggregates of acid groups.

High-Temperature Processes. Use of the derivative formalism to remove conduction losses facilitates the observation of relaxation processes (Figure 8a) at temperatures higher than T_g and frequencies 4−7 decades below the segmental relaxation. There are several possible origins of these processes: electrode polarization (EP), Maxwell−Wagner−Sillars interfacial polarization (MWS), and the so-called α* process involving association dynamics.[34,35]

EP, a phenomenon where mobile ions accumulate at the electrode interface,[36] can be ruled out as a possible source, as it is generally accompanied by a several order of magnitude

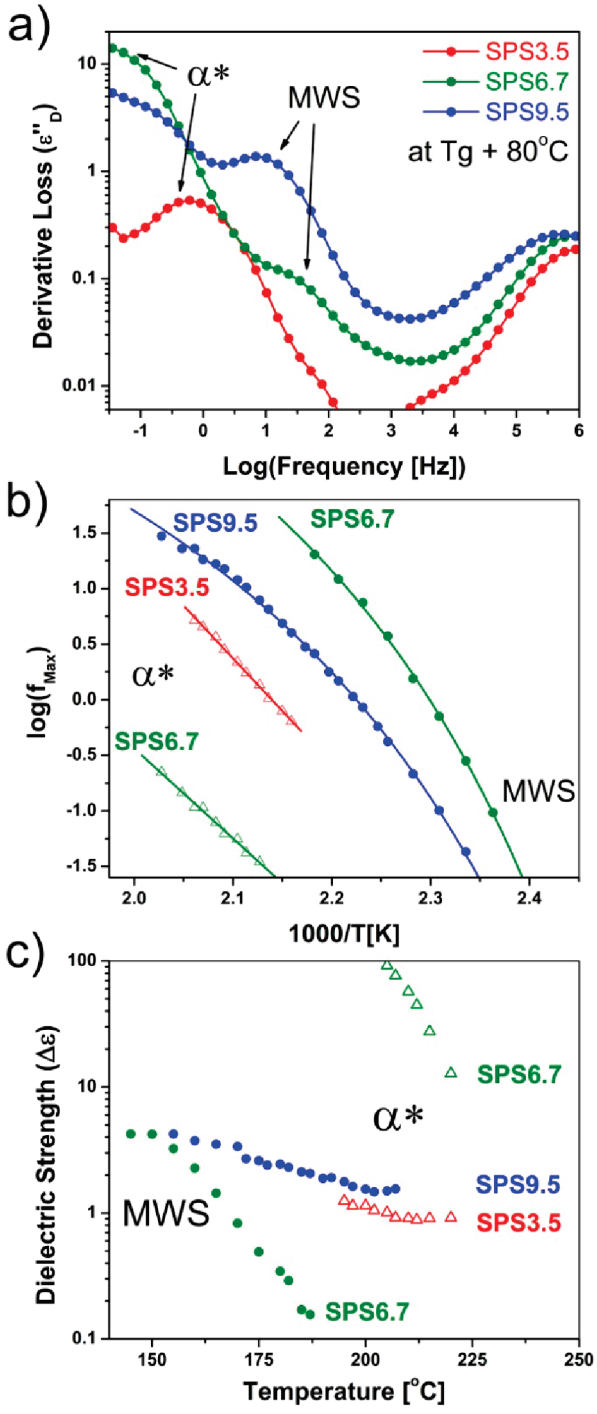

Figure 8. (a) Conduction free loss data for SPS3.5, 6.5, and 9.5 at $T_g + 80$ °C. Lines are shown to guide the eye. Temperature dependence of the (b) relaxation frequencies and (c) dielectric strength of the MWS (filled circles) and α* (open triangles) processes. Fits to the VFT and Arrhenius (lines) equations are included.

increase in the real part of the dielectric constant at low frequencies,[37] which is not observed in our experiments. The origin of MWS is similar to that of EP, where charge accumulation occurs at the interface in heterogeneous materials.[31,38] Since SPS6.5 and SPS9.5 are clearly microphase separated, we expect to observe MWS. α* is a "chemical" relaxation which has been attributed to the association and disassociation of hydrogen-bonded "stickers".[34,35] Although definitive assignment is difficult due to the limited temperature window in which they are observed, the experimental evidence points to

MWS and α* as origins of these high-temperature relaxations in SPS acid copolymers.

The MWS process has been studied for emulsions, multiphase blends, block copolymers, filled, and semicrystalline polymers.[31] This process generally has a temperature coefficient or activation energy which reflects that of dc conduction.[38] The temperature coefficient derived from fitting the dc conductivity (arising from ionic impurities, see Supporting Information) and the relaxation time of the MWS relaxation process (Figure 8b) to the VFT equation are within error for SPS9.5, which supports the assignment of this process as originating from interfacial polarization. The strength of this process (Figure 8c) is roughly the same at low temperatures for SPS6.5 and SPS9.5, which then drops off with increasing temperature. This is likely a result of the interfacial boundary between the proposed assemblies of sulfonic acid groups and the PS matrix becoming more diffuse with increasing temperature. Similarly, the low angle peak from X-ray scattering was found to increase in breadth with increasing temperature (Figure 4), indicating that the acid assemblies are no longer static and well-defined. An MWS relaxation was not observed for SPS3.5, which showed the weakest evidence of microphase separation.

The high-temperature dielectric relaxation for SPS3.5 and the second process observed for SPS6.5 (~180−220 °C), α* in Figure 8a, is in a similar temperature and frequency range as the high-temperature peak in the DMA loss modulus for similar SPS ionomers and acid copolymers.[5,10−13] This mechanical relaxation has been ascribed in previous studies to the dynamic glass transition temperature of the microphase-separated ion-rich phase; segmental motion of this phase requires the dissociation of dipole interactions.[5,10−13] The origin of this process in DRS cannot be ascribed to the segmental motion of the restricted cluster phase as the dielectric strength (Figure 8c) is significantly higher than that of the polystyrene segmental process, which would be the primary contributor to the strength of this process if this were the case. It is more likely that the molecular origin is comparable to the disassociation/association α* process observed in hydrogen-bonded thermoreversible networks; however, in the case of SPS acid copolymers, the "stickers" are comprised of dimers and larger assemblies of sulfonic acid groups. In the accessible temperature range this process appears to be Arrhenius-like with activation energies between 160 and 180 kJ/mol (Figure 8b). Its strength is significantly higher for SPS6.7 than SPS3.5 (Figure 8c), as expected for an acid copolymer with more and better formed acid assemblies. In both cases, the strength decays with temperature as the ionic associations becomes less favorable due to increased thermal energy. For SPS9.5 the α* process is expected to lower frequencies and higher temperatures than those measured in our experimental window.

Summary

X-ray scattering revealed the association of sulfonic acid groups that exhibited sensitivity to both processing conditions and temperature. The dynamics of these copolymers from DRS was found to be quite complex and to indicate the presence of acid−acid assembly. The relaxation time of the segmental relaxation increases with increasing sulfonic acid content along with the dielectric strength, consistent with an increasing number density of dipoles. The strength, however, was significantly lower than the calculated limiting case value from the Onsager equation assuming all dipoles were contributing and noninteracting. Calculation of the Kirkwood−Fröhlich interaction parameter revealed a reduction of net dipole moment due to antiparallel correlations and that the acid associations are thermally more stable at higher acid contents. These analyses of the characteristic segmental relaxation provide strong evidence of acid−acid assembly in these copolymers. Two high-temperature processes were identified at frequencies 4−7 decades below the segmental process. These processes are proposed to originate from MWS interfacial polarization and disassociation/reassociation dynamics of H-bonded dimers acid assemblies, also called the α* process. Future papers on the structure and dynamics of the neutralized versions of these acid copolymers as a function of counterion type and degree of neutralization will provide additional insight into the connection between aggregation and the complex dynamics of these materials.

Acknowledgment. This research was supported by the U.S. Department of Energy, Office of Basic Energy Sciences, Division of Materials Sciences and Engineering, under Award DEFG02-07ER46409 and by the NSF, Polymer Program, under Award NSF05-49116. We also thank Dr. Kevin Masser and Dr. Paul Painter for their helpful discussions as well as Dr. Wenjuan Liu for her contribution.

Supporting Information Available: Evidence supporting absence of thermal degradation, glassy state dynamics, VFT fit parameters of the relaxation time of the segmental relaxation, and dc conductivity. This material is available free of charge via the Internet at http://pubs.acs.org.

References and Notes

(1) Eisenberg, A.; Kim, J.-S. *Introduction to Ionomers*; Wiley: New York, 1998.
(2) Grady, B. P. *Polym. Eng. Sci.* **2008**, *48*, 1029–1051.
(3) Earnest, T. R.; Higgins, J. S.; Handlin, D. L.; MacKnight, W. J. *Macromolecules* **1981**, *14*, 192–196.
(4) Yarusso, D. J.; Cooper, S. L. *Macromolecules* **1983**, *16*, 1871–1880.
(5) Weiss, R. A.; Lefelar, J. A. *Polymer* **1986**, *27*, 3–10.
(6) Ding, Y. S.; Hubbard, S. R.; Hodgson, K. O.; Register, R. A.; Cooper, S. L. *Macromolecules* **1988**, *21*, 1698–1703.
(7) Zhou, N. C.; Chan, C. D.; Winey, K. I. *Macromolecules* **2008**, *41*, 6134–6140.
(8) Weiss, R. A.; Hongying, Z. *J. Rheol.* **2009**, *53*, 191–213.
(9) Colby, R. H.; Zheng, X.; Rafailovich, M. H.; Sokolov, J.; Peiffer, D. G.; Schwarz, S. A.; Strzhemechny, Y.; Nguyen, D. *Phys. Rev. Lett.* **1998**, *81*, 3876.
(10) Weiss, R. A.; Fitzgerald, J. J.; Kim, D. *Macromolecules* **1991**, *24*, 1071–1076.
(11) Weiss, R. A.; Yu, W. C. *Macromolecules* **2007**, *40*, 3640–3643.
(12) Atorngitjawat, P.; Klein, R. J.; Runt, J. *Macromolecules* **2006**, *39*, 1815–1820.
(13) Atorngitjawat, P.; Runt, J. *Macromolecules* **2007**, *40*, 991–996.
(14) Zhou, N. C.; Xu, C.; Burghardt, W. R.; Composto, R. J.; Winey, K. I. *Macromolecules* **2006**, *39*, 2373–2379.
(15) Heiney, P. A. *Comm. Powder Diffr. Newsl.* **2005**, *32*, 9–11.
(16) Kinning, D. J.; Thomas, E. L. *Macromolecules* **1984**, *17*, 1712–1718.
(17) Benetatos, N. M.; Heiney, P. A.; Winey, K. I. *Macromolecules* **2006**, *39*, 5174–5176.
(18) Percus, J. K.; Yevick, G. J. *Phys. Rev.* **1958**, *110*, 1–13.
(19) Fournet, G. *Acta Crystallogr.* **1951**, *4*, 293–301.
(20) Benetatos, N. M.; Chan, C. D.; Winey, K. I. *Macromolecules* **2007**, *40*, 1081–1088.
(21) van Turnhout, J.; Wubbenhorst, M. *J. Non-Cryst. Solids* **2002**, *305*, 50–58.
(22) Wubbenhorst, M.; van Turnhout, J. *J. Non-Cryst. Solids* **2002**, *305*, 40–49.
(23) Zundel, G. *Hydration and Intermolecular Interaction: Infrared Investigations with Polyelectrolyte Membranes*; Academic Press: New York, 1969.
(24) Ayyagari, C.; Bedrov, D.; Smith, G. D. *Macromolecules* **2000**, *33*, 6194–6199.
(25) Seitz, M. E.; Chan, C. D.; Opper, K. L.; Baughman, T. W.; Wagener, K. B.; Winey, K. I. *J. Am. Chem. Soc.* **2010**, *132*, 8165–8174.

(26) Santangelo, P. G.; Roland, C. M. *Macromolecules* **1998**, *31*, 4581–4585.
(27) Hodge, I. M. *J. Non-Cryst. Solids* **1996**, *202*, 164–172.
(28) Zhang; Painter, P. C.; Runt, J. *Macromolecules* **2002**, *35*, 8478–8487.
(29) Alexandrovich, P. S.; Karasz, F. E.; MacKnight, W. J. *J. Macromol. Sci., Part B* **1980**, *17*, 501–516.
(30) Liu, W. Unpublished results.
(31) Kremer, F.; Schonhals, A. *Broadband Dielectric Spectroscopy*; Springer-Verlag: Berlin, 2003.
(32) McCrum, N. G.; Read, B. E.; Williams, G. *Anelastic and Dielectric Effects in Polymeric Solids*; John Wiley & Sons Ltd.: New York, 1967.
(33) Zundel, G. *Angew. Chem., Int. Ed. Engl.* **1969**, *8*, 499–509.
(34) Müller, M.; Fischer, E. W.; Kremer, F.; Seidel, U.; Stadler, R. *Colloid Polym. Sci.* **1995**, *273*, 38–46.
(35) Muller, M.; Stadler, R.; Kremer, F.; Williams, G. *Macromolecules* **1995**, *28*, 6942–6949.
(36) Macdonald, J. R. *Phys. Rev.* **1953**, *92*, 4–17.
(37) Klein, R. J.; Zhang, S.; Dou, S.; Jones, B. H.; Colby, R. H.; Runt, J. *J. Chem. Phys.* **2006**, *124*, 144903.
(38) North, A. M.; Pethrick, R. A.; Wilson, A. D. *Polymer* **1978**, *19*, 913–922.